

SUPPLEMENTARY INFORMATION

Desmin- and vimentin-mediated hepatic stellate cell-targeting radiotracer ^{99m}Tc-GlcNAc-PEI for liver fibrosis imaging with SPECT

Deliang Zhang¹, Rongqiang Zhuang¹, Zhide Guo¹, Mengna Gao¹, Lumei Huang¹, Linyi You¹, Pu Zhang¹, Jindian Li¹, Xinhui Su², Hua Wu³, Xiaoyuan Chen⁴ and Xianzhong Zhang^{*,1}

1. State Key Laboratory of Molecular Vaccinology and Molecular Diagnostics & Center for Molecular Imaging and Translational Medicine, School of Public Health, Xiamen University, Xiamen 361102, China.
2. Department of Nuclear Medicine, Zhongshan Hospital affiliated to Xiamen University, Xiamen 361004, Fujian, China.
3. Department of Nuclear Medicine, The First Affiliated Hospital of Xiamen University, Xiamen 361003, China.
4. Laboratory of Molecular Imaging and Nanomedicine, National Institute of Biomedical Imaging and Bioengineering, National Institutes of Health, Bethesda, Maryland, 20892 USA.

* For correspondence contact:

Xianzhong Zhang, Professor, PhD
School of Public Health, Xiamen University
Xiang'an South Rd., Xiang'an district, Xiamen 361102, China.
Phone/Fax: +86(592)2880645;
E-mail: zhangxzh@xmu.edu.cn.

Supplementary methods

Dynamic SPECT/CT Imaging

SPECT/CT imaging was performed using nanoScan SC (Mediso Medical Imaging System). The CT acquiring parameters were as follows: energy peak of 50 kV, 670 μ A, 480 projections, medium zoom. SPECT acquiring parameters were as follows: energy peak of 140 keV for ^{99m}Tc , window width of 20 %, matrix of 256 \times 256, medium zoom, and frame: 30 s. Dynamic SPECT acquiring parameters were as follows: 25 scans, and 20 sec/frame from 0 to 50 min.

Supplementary Figures

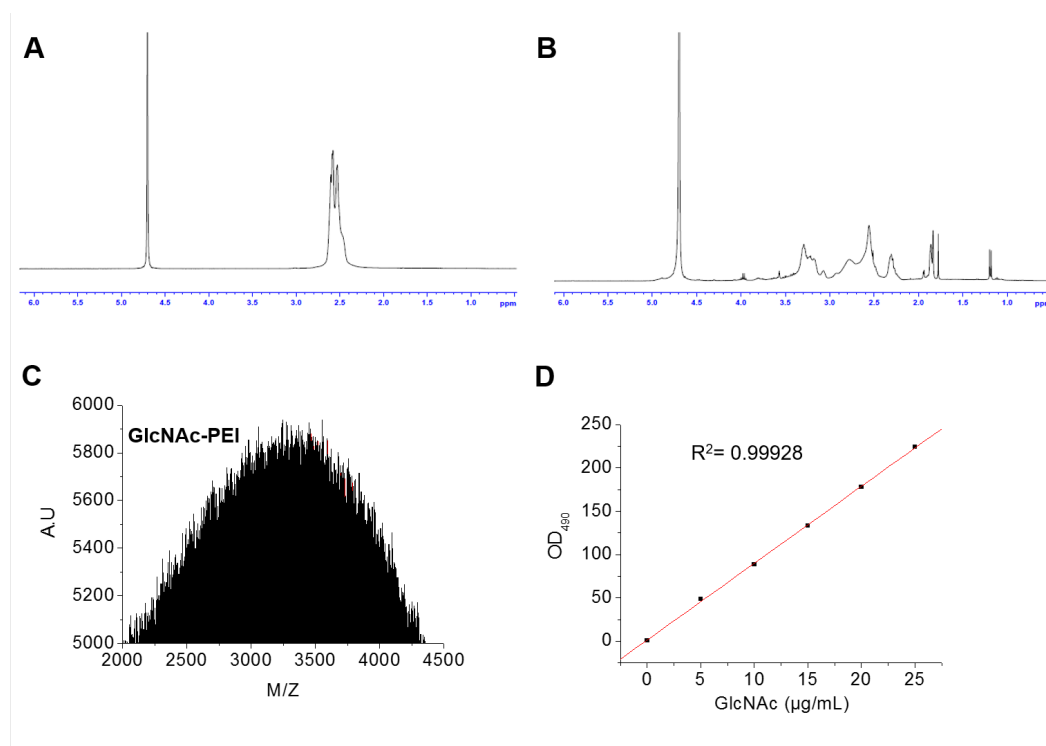


Fig. S1. (A) ¹H-NMR spectra of PEI-1800. (B) ¹H-NMR spectra of GlcNAc-PEI (showed a characteristic absorbance peak of COCH₃ in 1.81-1.88 ppm). (C) MODI-TOF-MS of GlcNAc-PEI. (D) Standard curve showing the absorbance of different concentrations of GlcNAc by phenol-vitriol method.

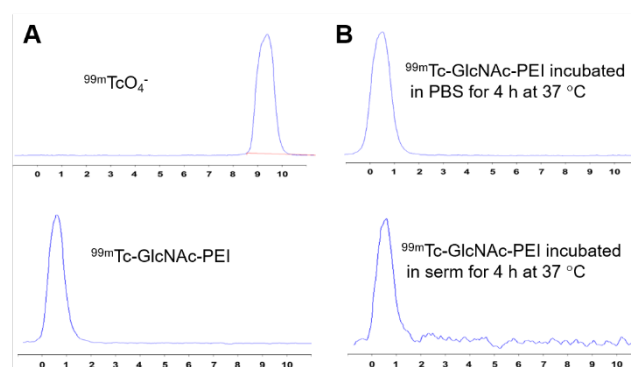


Fig. S2. (A) The TLC results of ^{99m}TcO₄⁻ and ^{99m}Tc-GlcNAc-PEI. (B) The in vitro stability results of ^{99m}Tc-GlcNAc-PEI after incubated in PBS or serum for 4 h at 37 °C.

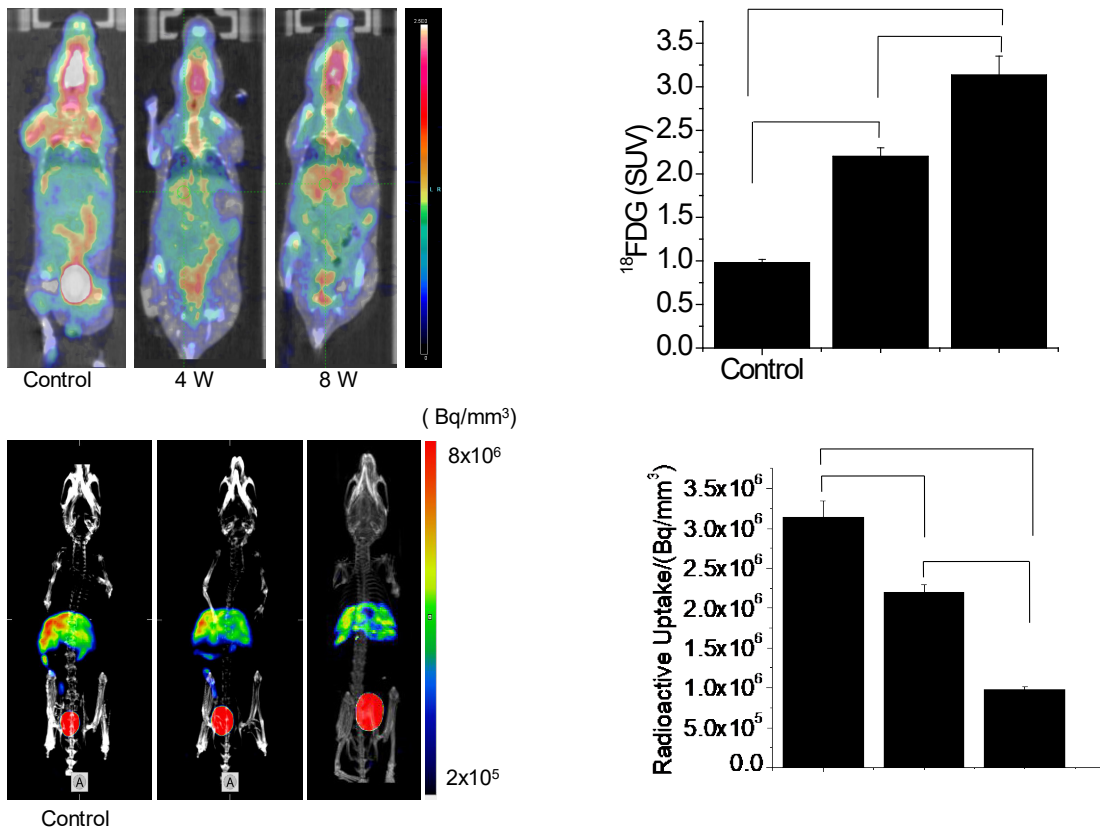


Fig. S3. (A) ^{18}F -FDG PET/CT imaging of control and fibrotic mice. (B) Liver uptake of ^{18}F -FDG by drawing ROI of the whole liver. (C) $^{99\text{m}}\text{Tc}$ -GSA SPECT/CT imaging of control and fibrotic mice. (D) Liver uptake of $^{99\text{m}}\text{Tc}$ -GSA by drawing ROI of the whole liver.

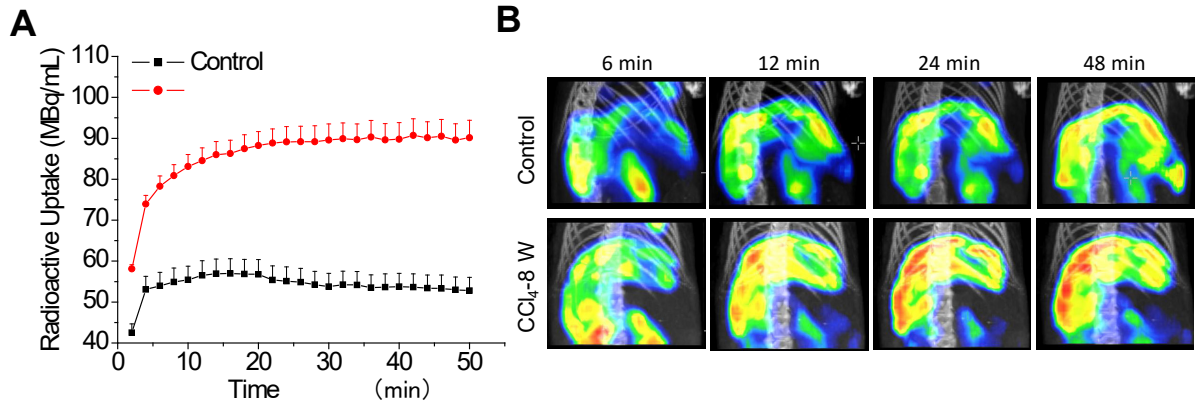


Fig. S4. (A) The time-activity curves derived from the dynamic SPECT imaging of control and fibrotic mice. (B) Representative images of ^{99m}Tc-GlcNAc-PEI dynamic SPECT imaging of control and fibrotic mice.

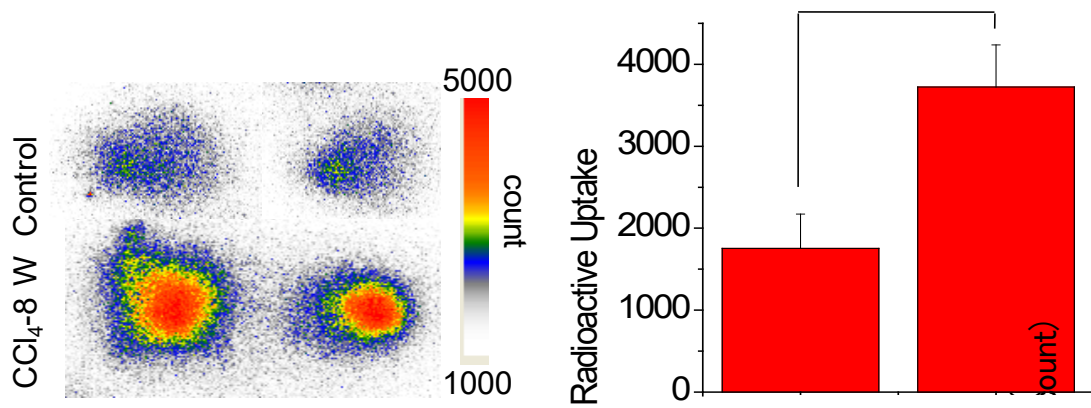


Fig. S5. Autoradiography of control and fibrotic liver tissues with ^{99m}Tc-GlcNAc-PEI.

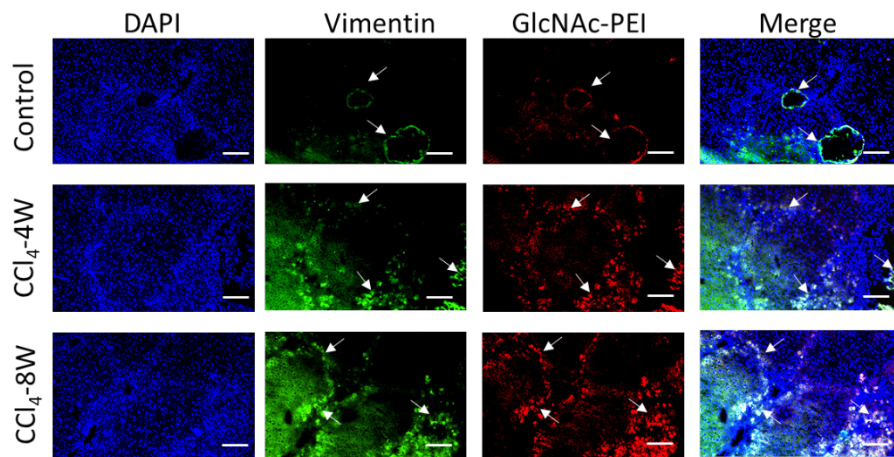


Fig. S6. Immunofluorescence co-localization analysis of vimentin and GlcNAc-PEI-Cy5.5 in the liver tissue of CCl₄-induced fibrotic mice. Blue: DAPI; green: anti-vimentin staining FITC; Red: GlcNAc-PEI-Cy5.5. Scale bar: 200 μ m.

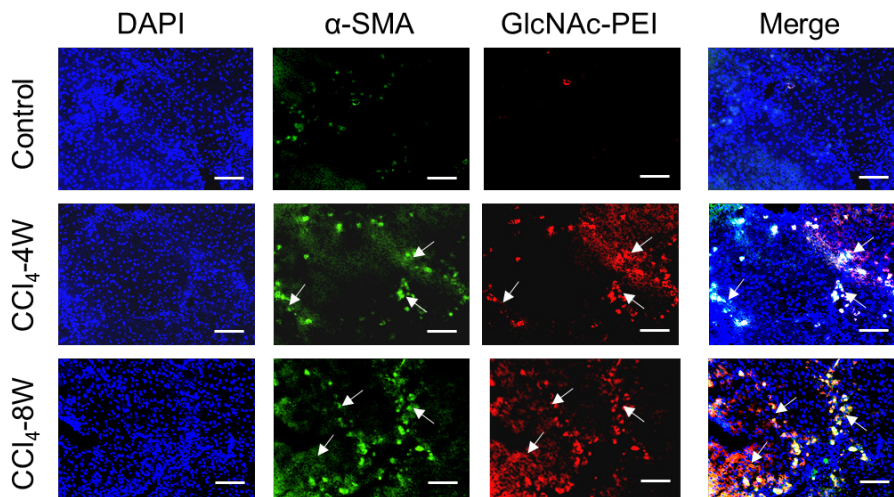


Fig. S7. Immunofluorescence co-localization analysis of α -SMA and GlcNAc-PEI-Cy5.5 in the liver tissue of CCl₄-induced fibrotic mice. Blue: DAPI; green: anti- α -SMA staining FITC; Red: GlcNAc-PEI-Cy5.5. Scale bar: 200 μ m.

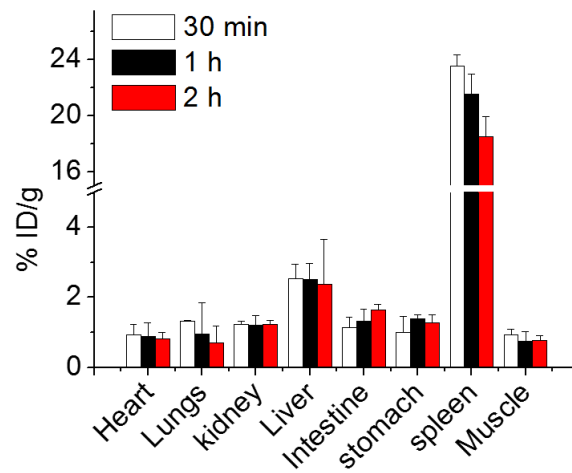


Fig. S8. Biodistribution of ^{99m}Tc -GlcNAc-PEI in the normal mice.

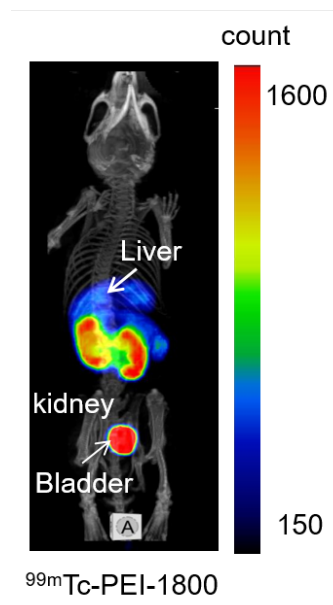


Fig. S9. SPECT/CT imaging of fibrotic mice with nontargeting ^{99m}Tc -PEI-1800.

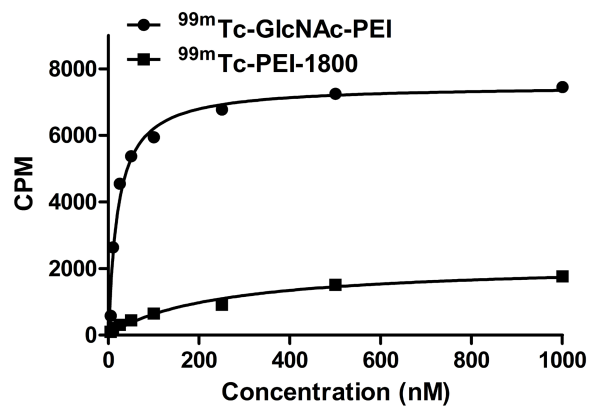


Fig. S10. Saturation binding assay of ^{99m}Tc -GlcNAc-PEI with vimentin protein.

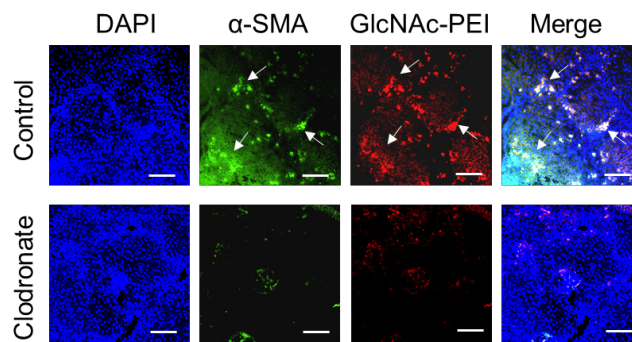


Fig. S11. Immunofluorescence co-localization analysis of α -SMA and GlcNAc-PEI-Cy5.5 in the liver tissue of fibrotic mice after clodronate liposome treatment. Blue: DAPI; green: anti- α -SMA staining FITC; Red: GlcNAc-PEI-Cy5.5. Scale bar: 200 μm .